Biochemical and Biophysical Research Communications 665 (2023) 195–201

Contents lists available at ScienceDirect

Biochemical and Biophysical Research Communications

journal homepage: www.elsevier.com/locate/ybbrc

Activated EGFR and PDGFR internalize in separate vesicles and downstream AKT and ERK1/2 signaling are differentially impacted by cholesterol depletion

Erik Wåhlén, Frida Olsson, Doroteya Raykova, Ola Söderberg, Johan Heldin[*], [1], Johan Lennartsson [1]

Department of Pharmaceutical Biosciences, Uppsala University, Husarg 3, SE-75124, Uppsala, Sweden

ARTICLE INFO

Article history:
Received 3 April 2023
Received in revised form
14 April 2023
Accepted 26 April 2023
Available online 3 May 2023

Keywords:
EGFR
EGF
PDGFR
PDGF
Membrane raft
Lipid rafts
Receptor tyrosine kinase
Internalization

ABSTRACT

The interplay between membrane subregions and receptor tyrosine kinases (RTK) will influence signaling in both normal and pathological RTK conditions. In this study, epidermal growth factor receptor (EGFR) and platelet-derived growth factor receptor β (PDGFR-β) internalizations were investigated by immunofluorescent microscopy following simultaneous treatment with EGF and PDGF-BB. We found that the two receptors utilize separate routes of internalization, which merges in a common perinuclear endosomal compartment after 45 min of stimulation. This is further strengthened when contrasting the recruitment of either EGFR or PDGFR-β to either clathrin or caveolin-1: PDGFR-β dissociates from caveolin-1 upon stimulation, and engages clathrin, whilst an increased recruitment of EGFR, to both clathrin and caveolin-1, was observed upon EGF stimulation. The association between EGFR and caveolin-1 is supported by the observation that EGFR was localized in lipid raft associated fractions, whereas PDGFR-β was not. We also found that disruption of lipid rafts using MβCD led to an increased EGFR dimerization and phosphorylation in response to ligand, as well as a dramatic decrease in AKT- and a smaller but robust decrease in ERK1/2 phosphorylation. This suggest that lipid rafts may be important to effectively connect the EGFR with downstream proteins to facilitate signaling. Our data implies that cholesterol depletion of the plasma membrane affect the signaling of EGFR and PDGFRβ differently.

1. Introduction

The epidermal growth factor receptor (EGFR) is a transmembrane surface protein that is part of the receptor tyrosine kinase (RTK) superfamily, and mediates cellular response to several external growth factors, e.g. epidermal growth factor (EGF), transforming-growth factor-α (TGFα), and the neuregulins [1]. EGFR belongs to a family of four structurally similar tyrosine kinase receptors called ErbB or HER. Namely, EGFR/HER1/ErbB1, Neu/HER2/ErbB2, HER3/ErbB3, and HER4/ErbB4 [2]. Ligand binding to the EGFR ectodomain will induce the receptors to homo- or heterodimerize, leading to increased activity of the intracellular tyrosine kinase domains [1,3–5]. The activation of the EGFR leads to the activation of several intracellular downstream cascades, such as: JAK/STAT, RAS/ERK1/2, and PI3K/AKT/mTOR pathways – promoting cell survival, migration, differentiation, and proliferation [2,6,7].

The platelet-derived growth factor receptor (PDGFR), also belonging to the RTK superfamily, with two different isoforms, i.e., PDGFR-α and PDGFR-β [8]. Similar to EGFR, ligand-induced dimerization of PDGFR leads to phosphorylation of intracellular tyrosine residues [8]. These phosphorylation sites allow for docking of signaling proteins to the activated receptor complex. Many of the signaling pathways activated by PDGFR overlap with those activated by EGFR. We have earlier reported a potential dependence of membrane rafts for certain PDGFR-β downstream signaling cascades to properly function in human fibroblasts, i.e., PI3K/AKT and RAS/ERK1/2 [9]. These membranal microdomains have also been linked to RTK internalization [10].

Internalization is an integral part in regulating RTK signaling, both temporally and spatially, and ultimately determines the receptors fate, whether it be recycled or degraded [11]. Upon activation, EGFR signaling takes place both at the plasma membrane

* Corresponding author.
E-mail address: johan.heldin@farmbio.uu.se (J. Heldin).
[1] authors have contributed equally.

https://doi.org/10.1016/j.bbrc.2023.04.099

and in endosomes [12]. A major internalization route of EGFR is via clathrin-coated pits, but it can also internalizes via clathrin-independent routes, which may be one or several pathways, where membrane rafts are believed to play an important role [11,13]. For instance, EGFR have previously been reported to internalize through caveolae, where the proteins caveolins have been reported as necessary for proper receptor function [14–16]. However, the understanding of the underlying mechanisms of these clathrin-independent routes are poor. It has been suggested that, depending on route of internalization, EGFR can be fated for either recycling, where internalization facilitated via clathrin-coated pits prompt recycling, and clathrin-independent internalization favors degradation [11]. It has also been suggested that certain signaling pathways, such as AKT and ERK1/2, require interaction with intact clathrin-coated pits for proper signaling, while others do not [11].

In this study we have investigated the differences in internalization between EGFR and PDGFR-β, and the potential implications this holds for EGFR and PDGFR-β signaling. Also, whether active PDGFR and EGFR sort together through endosomal compartments has been investigated. As EGFR is often used as a model system for endocytosis for other RTKs, it is of interest and importance to highlight any potential difference between these receptors [17].

2. Material & methods

2.1. Cell culture

The immortalized fibroblast cell line of human foreskin BJ-hTERT (kind gift from professor Carl-Henrik Heldin, Uppsala University) was cultured in Dulbecco's Modified Eagle Medium + GlutaMAX (DMEM + GlutaMAX) supplemented with 10% fetal bovine serum (FBS), all acquired from Thermo Fisher Scientific, at 37 °C and 5% CO_2.

2.2. Western blot

Western blot analysis was performed as described in Wåhlén et al. [9]. Cells were first seeded to a confluence of 50,000 cells/cm^2, and left to adhere overnight. Thereafter serum starved for 16 h in DMEM + GlutaMAX supplemented with 0.2% lipid free BSA (starvation medium). Cells were treated with 5 mM Methyl-β-Cyclodextrin (MβCD) for 3 h (freshly dissolved in serum starvation medium prior to the experiment) and stimulated with 20 ng/ml EGF for the last 0, 15, 30, 45, 60 min of the experiment. Stimulation was then terminated by washing the cells with ice-cold PBS on ice and afterward lysing the cells using 1.5 x NuPAGE™ LDS Sample Buffer supplemented with 20 mM dithiothreitol (DTT), and a protease and phosphatase inhibitor cocktail (PhosSTOP, 4906837001 and cOmplete, 4693159001, Sigma).

The lysate was boiled at 95 °C for 5 min, and then sample proteins were separated on SDS-polyacrylamide gel and afterward transferred to a PVDF-FL membrane, using Chameleon Duo Pre-Stained Protein Ladder (LI-COR Biosciences) as size reference. The transferred membrane was then washed in TBS, and blocked in Intercept blocking buffer (LI-COR Biosciences, diluted 1:3 in TBS) at room temperature for 2 h and subsequently incubated with primary antibodies at 4 °C over-night (Supplementary Table 1). Membranes were washed 3 × 10 min in TBS supplemented with 0.05% Tween-20 (TBS-T), and then incubated with appropriate secondary antibodies (Alexa680 or IRDye800) diluted in Intercept Blocking Buffer. The membranes were then washed again in TBS-T for 3 × 10 min. An Odyssey Scanner and ImageStudio v5.2.5 software (both from LI-COR Biosciences) was used for scanning and quantifications of the membranes.

2.3. Dimerization assay

Cells were seeded and starved, as described above, and pre-incubated with or without MβCD for 2 h, and then stimulated with 20 ng/ml EGF for either 0 or 5 min at 37 °C. The cells were washed in ice-cold PBS three times. 2 mM bis-sulfosuccinimidyl suberate (BS3, Thermo Fisher Scientific, 21,580) in ice-cold PBS was added to the cells, and they were incubated for 60 min on ice. To terminate cross-linking, cells were washed 3 × 5 min in ice-cold TBS. Cells were lysed and analyzed with western blot as described above.

2.4. Immunofluorescence microscopy (IF)

Cells were seeded, as described above, and starved over-night in DMEM + GlutaMAX supplemented with 0.2% FBS medium in an 8-well chamber slide. BJ-hTERTs were then stimulated with 20 ng/ml EGF and 20 ng/ml PDGF-BB, concurrently. Medium was aspirated and cells were then washed in ice-cold PBS, and fixed in 3,7% formaldehyde solution for 15 min on ice. Cells were washed 3 × 5 min in PBS, permeabilized with 0.2% Triton X-100 in TBS for 10 min. After blocking in Intercept blocking buffer (LI-COR Biosciences, diluted 1:3 in TBS) for 1 h at 37 °C, cells were incubated over-night at 4 °C with primary antibodies as described in Supplementary Table 1. The slides were then washed in TBS-T for 3 × 10 min, and incubated in Hoechst 33342 (5 μg/ml), donkey anti-rabbit (Alexa Fluor Plus 555, A32794) and donkey anti-goat (Alexa Fluor Plus 647, A32849) for 1 h at 37 °C. Slides were washed in TBS-T for 3 × 10 min, and mounted with SlowFade Gold antifade mountant (Thermofisher scientific, S36936).

2.5. Proximity ligation assay (PLA)

BJ-hTERT cells were seeded, as described above, and starved over-night in starvation medium in an 8-well chamber slide, and stimulated with either 20 ng/ml EGF or 20 ng/ml PDGF-BB for 0, 5, 15 or 45 min, respectively. Cells were then fixed and permeabilized, as described under the *Immunofluorescens microscopy* section. Proximity ligation assay was then performed according to the manufacturer's instructions (NaveniFlex MR, Navinci Diagnostics), a more efficient version of *in situ* PLA [18]. Primary antibodies used are described in Supplementary Table 1.

2.6. Sucrose fractionation

Cells were seeded and starved as described above, and stimulated either with 20 ng/ml EGF or PDGF-BB for 15 min at 37 °C, respectively. The enrichment for raft associated proteins was then proceeded with as described by Gajate & Mollinedo, with minor modifications to the protocol [19]. Medium was aspirated and cell were washed in ice-cold PBS. Cells were then collected by scraping in 2 ml TNEV buffer (150 mM NaCl, 5 mM EDTA, 10 mM Tris-HCl, pH 7.5) supplemented with protease inhibitor (cOmplete, 4693159001, Sigma). The cells were pelleted at 300×*g* for 7 min, after which the supernatant was aspirated and cells were washed in 10 ml ice-cold PBS, and centrifuged at 300×*g* for 7 min. The wash and centrifugation were repeated once more. The supernatant was aspirated and 1.4 ml of 1% Triton X-100 in TNEV buffer was added to the pellet, which was then re-suspended, and left to incubate for 1 h at 4 °C. Cells were homogenized with 20 strokes through a 21 G needle, and centrifuged at 200×*g* for 8 min. The supernatant was saved, whilst the pellet containing unbroken cells, cellular debris and nuclei was discarded. 1 ml of the supernatant was mixed with 1 ml 85% sucrose (w/v) in TNEV buffer solution, and transferred to a pre-chilled 14 × 95-mm Polypropylene round-bottom centrifuge tubes. 6 ml 35% (w/v) sucrose solution in TNEV buffer and then 3.5 ml 5% (w/v) sucrose solution in TNEV buffer was then carefully overlaid the mixture, forming a discontinuous gradient. The samples were centrifuged in a SW40 Ti at 35,000 rpm (200,000 g, at r_{max}) for 18 h at 4 °C. 1 ml fractions were collected from the top and mixed with 4 x NuPAGE™ LDS Sample Buffer to a final concentration of 1.5 x NuPAGE™ LDS Sample Buffer supplemented with 20 mM dithiothreitol (DTT), and a protease and phosphatase inhibitor cocktail (PhosSTOP, 4906837001 and cOmplete, 4693159001, Sigma). The fractions were analyzed with western blot, as described above.

2.7. Imagining and image analysis

With the Zeiss imager M2 microscope and Zen 2 (blue edition), at least three, or more, pictures were acquired per experimental condition with a 40X/1.4 or 63X/1.4 oil objective and Hamamatsu C11440 camera. For sample excitation, the light source HXP 120 V (90% intensity), was used. Cube filter sets 31, 43HE, 49, and 50 (Zeiss) were used, which are suitable for TexRed, Hoechst 33342, Alexa Fluor Plus 555, Alexa Fluor Plus 647 fluorophores. All images were deconvolved prior image analysis as described in Raykova et al. [20]. Cell profiler 3.1.9 was used for image quantification and analysis, on deconvolved images. Signal strength has been enhanced for visualization purposes for IF and PLA figures.

2.8. Statistical analysis

Experiments were independently repeated at least three times and analyzed with Graphpad Prism 9. Normal distribution of the data was determined with Shapiro-Wilks test. Non-parametric one-way ANOVA (Kruska-Wallis test) was used in analyzing the PLA and IF data. Non-parametric Mann-Whitney test was used to analyze the Western blot and Dimerization assay data.

2.9. Mycoplasma

Cells were analyzed for mycoplasma contamination twice a year with PCR.

3. Results & discussion

In order to investigate the role of membrane rafts for EGFR-signaling, we treated BJ-hTERT cells with MβCD to reduce levels of cholesterol. After cholesterol extraction, BJ-hTERT cells were analyzed with western blot for activation of EGFR and downstream signaling (Fig. 1). We found that total levels of EGFR in BJ-hTERT cells were unaffected by the MβCD treatment, as compared to controls (Fig. 1A–B). The phosphorylation of tyrosine residue 1068 in the EGFR (pY1068-EGFR) was however significantly increased by approximately 60% in cells treated with MβCD after 30 min of stimulation with 20 ng/ml EGF (Fig. 1A and C). In addition, an overall increase in pY1068-EGFR, however, not significant was observed at all other time-points in cells treated with MβCD compared to controls. The increased receptor phosphorylation may be explained by the 2.5 times increased dimerization of EGFR after 5 min of EGF stimulation and MβCD treatment, as compared to control (Fig. 1D–E). This observation that lipid rafts inhibit EGFR dimerization is consistent with reports that EGFR upon stimulation moves out of lipid rafts to become dimerized [21,22].

The increased phosphorylation and dimerization of EGFR is in contrast to our previous data on PDGFR-β in the same cell line, where we did not see such an effects on the receptor (Fig. 1F and [9]).

Downstream of EGFR, phosphorylation of AKT and ERK1/2 was analyzed by western blot, after treatment with 5 mM MβCD and stimulation with 20 ng/ml EGF. Phosphorylation of serine residue 473 on AKT (pS473-AKT) was abolished in cells treated with MβCD compared to the controls (Fig. 1A and G). Similarly, phosphorylation of threonine residue 202 and tyrosine residue 204 on ERK1/2 (pT202/Y204-ERK1/2) were significantly decreased in cells treated with MβCD, compared to the untreated control (Fig. 1A and H). Interestingly, we found a marked effect on EGF-induced pS473-AKT in cells treated with MβCD, while only a mild effect was observed in PDGF-stimulated cells and vice versa for ERK1/2 (Fig. 1 and [9]). The differences in receptor activation between EGFR and PDGFR-β, as well as, the differences in downstream signaling implies that the two receptors have different requirements of the cholesterol in the membrane for initiating signal transduction.

The differences in signal transduction led us to investigate if activated PDGFR-β and EGFR were internalized and sorted differently. To this end, we simultaneous stimulated cells with 20 ng/mL of EGF and PDGF-BB for 0, 15 and 45 min and trafficking of EGFR and PDGFR-β was observed by immunofluorescence (Fig. 2). Low levels of co-localization was observed between EGFR and PDGFR-β, either after 0 and 15 min of stimulation (Pearson coefficient <0.5, considered not to co-localize). The two receptors have a low level of co-localization at the plasma membrane prior to ligand stimulation. However, after stimulation the degree of co-localization between the two receptors increased to reach a Pearson coefficient >0.5 after 45 min of stimulation (Pearson coefficient >0.5, considered co-localization), likely corresponding to their entry to perinuclear compartments. It is therefore likely that upon simultaneous activation of EGFR and PDGFR-β the two receptors are at least in part trafficked separately into early/recycling endosomal compartments, and then a larger portion coalesce in late endosomes/multivesicular bodies or lysosomal compartments. This separate trafficking may allow for interaction with signaling proteins in a specific manner (qualitatively or quantitatively), potentially explaining the difference we observe in AKT and ERK1/2 phosphorylation in cells stimulated with PDGF-BB or EGF (Fig. 1 and [9]).

To investigate to what degree PDGFR-β and EGFR are recruited to different plasma membrane compartments during internalization, such as clathrin-coated pits or caveolin-1 enriched lipid rafts, proximity ligation assays were used to study receptor specific recruitment to clathrin and caveolin-1. EGFR showed a rapid but transient recruitment to clathrin-coated pits, which peaked at 5 min (Fig. 3A–B). PDGFR-β showed comparable kinetics to EGFR, and the recruitment of PDGFR-β to clathrin-coated pits peaked between 5 and 15 min of stimulation (Fig. 3C–D). This is indicative of both EGFR and PDGFR-β using clathrin-mediated internalization pathways, as has also been previously shown [23].

Receptor proximity to caveolin-1 was also investigated. EGFRs recruitment to caveolin-1 increased upon stimulation, peaking after 15 min of stimulation (Fig. 3E–F). PDGFR-β, on the other hand, shows a clear association with Caveolin-1 in unstimulated cells but this association decreases significantly in response to PDGF-BB treatment (Fig. 3G–H), which is in concordance with a study showing PDGFR-β is held inactive in caveolae [24] and thus needs to leave the caveolae to be activated in non-raft plasma membrane. This suggests that a fraction of the PDGFR-β population on the membrane is held close to Caveolin-1 in unstimulated cells but leaves them and is primarily internalized via clathrin-mediated endocytosis in response to PDGF stimulation, whereas EGFR utilizes membrane raft and caveolae-associated pathways in addition to clathrin-mediated internalization.

To further investigate the differences between PDGFR-β and EGFR localization we used sucrose gradient fractionation where membrane raft associated proteins were enriched in lower density fractions (Fig. 4; fraction 2–4), which was validated using the membrane raft marker proteins caveolin-1 and flotillin-2.

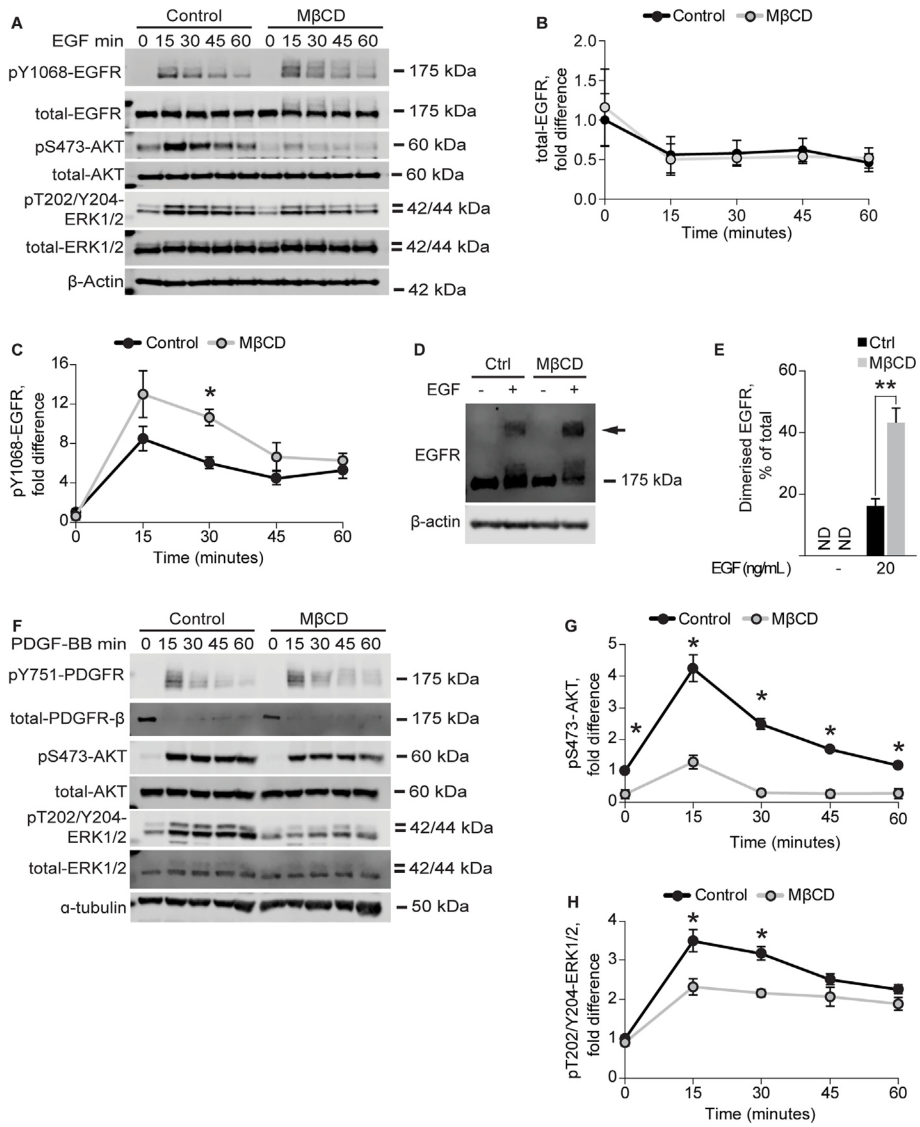

Fig. 1. EGFR activation increases upon cholesterol depletion, but downstream activation of AKT and ERK1/2 is reduced. BJ-hTERT cells were incubated with or without 5 mM MβCD for 3 h, and stimulated with 20 ng/ml EGF during the last hour for either 0, 15, 30, 45 or 60 min at 37 °C, and analyzed with western blot using antibodies specific against specific phosphorylation sites and total EGFR, AKT, ERK1/2 and β-actin (A). Quantifications of total EGFR, phosphorylation of tyrosine residue 1068 of EGFR (B, C), serine residue 473 of AKT (G), and threonine residue 202 and tyrosine residue 204 of ERK1/2 (H) are shown, respectively. BJ-hTERT cells were pre-incubated with 5 mM MβCD for 2 h, and stimulated with 20 ng/ml EGF for 0 or 5 min at 37 °C, and then cross-linked with BS3, to determine levels of receptor dimerization. This was then analyzed with western blot with antibodies specific against total EGFR and β-actin (D, dimerized receptor indicated with an arrow) and quantifications are shown in (E). The total EGFR stain has been normalized to β-actin levels, and all phosphorylation stains were normalized to respective total protein stain, and fold difference was determined by dividing with the mean of all 0 min values, excluding MβCD. Cross-linked EGFR was normalized to total EGFR levels in the dimerization assay. Error bars represents the standard error of the mean (SEM). $n \geq 4$ for all above experiments; * = $p \leq 0.05$, ** = $p \leq 0.01$. BJ-hTERT cells were also incubated with or without 5 mM MβCD for 3 h, and stimulated with 20 ng/ml PDGF-BB at the last hour for either 0, 15, 30, 45 or 60 min at 37 °C, and analyzed with western blot with antibodies targeting specific phosphorylation sites and total PDGFR-β, AKT, ERK1/2 and β-actin (F); $n = 1$.

PDGFR-β was not found in the fractions corresponding to membrane rafts, instead localized in higher density fractions, which interestingly were also enriched in Caveolin-1 (Fig. 4; fraction 6–12). This is consistent with our PLA data showing clear proximity between PDGFR-β and Caveolin-1 in unstimulated cells. In response to PDGF-BB treatment, PDGFR-β is further enriched in the highest density fractions (Fig. 4; fraction 10–12). It is currently unclear what cellular compartment these fractions represent, but since they are also enriched in α-tubulin they may be cytosolic fractions containing vesicles, some of which are rich in Caveolin-1 as well as internalized receptors. Furthermore, these heavier density fractions are also enriched in EEA1, Calreticulin and GM130, and thus these fractions also likely correspond to early endosomal compartments, endoplasmic reticulum or golgi. Despite being in fractions with similar density, our PLA data suggests that PDGFR-β and Caveolin-1 are separated in response to PDGF-BB treatment (Fig. 3).

EGFR was found in both lower- and higher density fractions, suggesting a direct association with membrane rafts at steady-state levels, but not an exclusive residence within these domains. These variations in receptor localization may further explain the differences in their internalization, where certain internalization pathways have been associated to membrane rafts (Fig. 4).

Collectively, we have found that EGFR and PDGFR-β partly uses different internalization pathways; PDGFR primarily internalizes via clathrin coated pits, whereas EGFR in addition can be

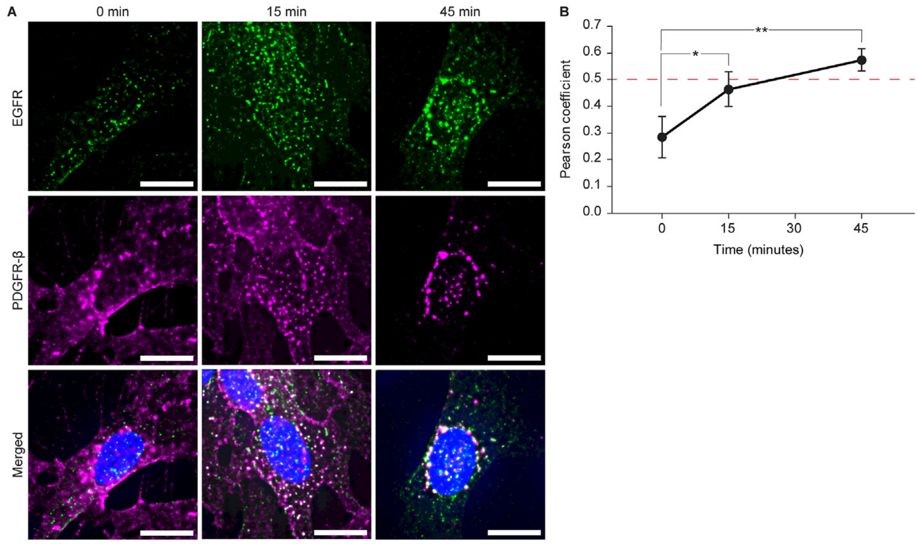

Fig. 2. EGFR and PDGFR deviate in internalization pathways. EGFR and PDGFR-β localization in BJ-hTERT upon simultaneous stimulation with EGF (20 ng/ml) and PDGF-BB (20 ng/ml) for 0, 15 or 45 min at 37 °C was investigated with immunostaining. A Pearson coefficient of >0.5 indicates co-localization (indicated in figure with a dashed line). Nuclei are shown in blue, EGFR in green, and PDGFR-β in magenta. Error bars represents the standard error of the mean (SEM). $n = 3$ for all experiment; scale bar = 5 μm; * = $p \leq 0.05$, ** = $p \leq 0.01$. (For interpretation of the references to colour in this figure legend, the reader is referred to the Web version of this article.)

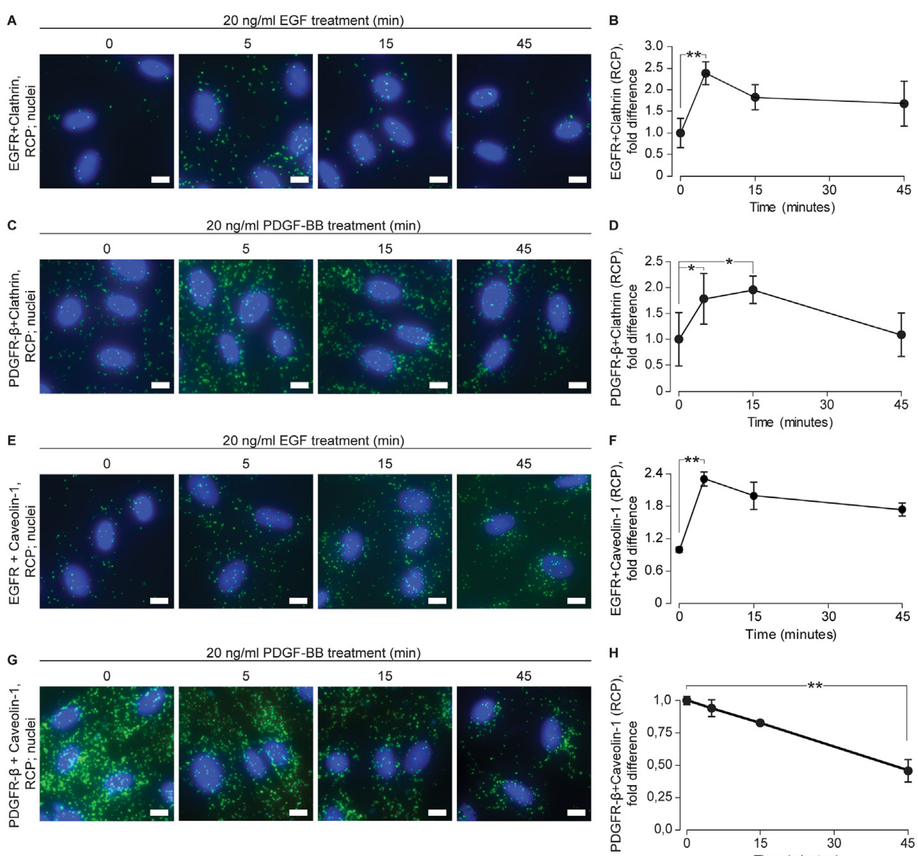

Fig. 3. EGFR and PDGFR both internalize via clathrin coated pits, but deviate in clathrin-independent endocytosis pathways. To investigate potential differences in internalization routes of EGFR and PDGFR-β, co-localization with clathrin or caveolin-1 was investigated using proximity ligation assay (PLA) after stimulation with 20 ng/ml EGF or PDGF-BB. The co-localization between Clathrin and EGFR or PDGFR-β is shown in (A or C) and quantified in (B or D), respectively. Co-localization between Caveolin-1 and EGFR or PDGFR-β is shown in (E or G) and quantified in (F or H), respectively. Nuclei are shown in blue, and PLA rolling circle amplification product (RCP) in green. Error bars represents the standard error of the mean (SEM). $n \geq 4$ for all experiment; scale bar = 10 μm; * = $p \leq 0.05$, ** = $p \leq 0.01$. (For interpretation of the references to colour in this figure legend, the reader is referred to the Web version of this article.)

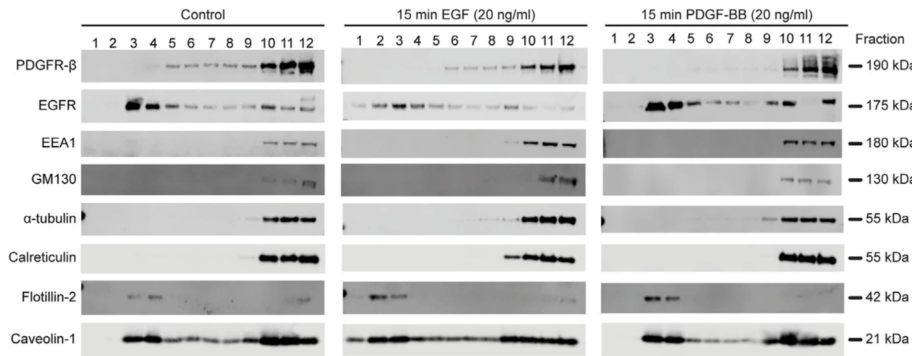

Fig. 4. EGFR but not PDGFR is enriched in low sucrose density fractions, together with the lipid raft markers flotillin-2 and caveolin-1. Membrane raft associated proteins have been found to be enriched in lower density sucrose fractions containing Flotillin-2 and Caveolin-1 after ultracentrifugation. BJ-hTERT cells were stimulated with either EGF or PDGF-BB (20 ng/ml, respectively) for 0 or 15 min at 37 °C, and cell lysates ultracentrifuged in a discontinuous sucrose gradient of 5, 35 and 42.5% (w/v) sucrose in TNEV buffer fraction, and analyzed with western blot. Lower density fractions are indicated with a lower number, and higher at a higher number, from 1 to 12. Membrane rafts associated proteins are expected to be found between fraction 2–4, and cytosol and non-raft membrane (including ER and Golgi) between fraction 6–12. n = 3 for all experiments.

internalizes via clathrin-independent pathways, such as via caveolae. This may explain the different effects on downstream signaling that was observed upon cholesterol extraction, and subsequent membrane raft disruption. It is possible that differences in receptor internalization routes influences access to different signaling protein complexes, which can expain the selective effects.

Funding

The study was funded by grants from the Swedish Cancer Society (J.L., 21 1427 Pj 01H & O.S., 22 2306 Pj).

CRediT author statement

Conceptualization, J.H. and J.L.; Validation, E.W. and F.O.; Formal Analysis, E.W. D.R. and F.O.; Investigation, E.W. and F.O.; Resources, O.S. and J.L.; Writing – Original Draft Preparation, J.H., E.W. and J.L.; Writing – Review & Editing, J.H., E.W., O.S. and J.L.; Visualization, F. O., D. R. and E.W.; Supervision, J.H. and J.L.; Project Administration, J.H.; Funding Acquisition, O.S. and J.L. All authors have read and approved the final version of the manuscript.

Declaration of competing interest

O.S. is inventor on the patent covering the UnFold PLA technology, commercialized by Navinci.

Appendix A. Supplementary data

Supplementary data to this article can be found online at https://doi.org/10.1016/j.bbrc.2023.04.099.

References

[1] R.N. Jorissen, F. Walker, N. Pouliot, T.P.J. Garrett, C.W. Ward, A.W. Burgess, Epidermal growth factor receptor: mechanisms of activation and signalling, Exp. Cell Res. 284 (2003) 31–53, https://doi.org/10.1016/S0014-4827(02)00098-8.
[2] A.A. Rosenkranz, T.A. Slastnikova, Epidermal growth factor receptor: key to selective intracellular delivery, Biochem 85 (2020) 967–993, https://doi.org/10.1134/S0006297920090011.
[3] S. Cohen, H. Ushiro, C. Stoscheck, M. Chinkers, A native 170,000 epidermal growth factor receptor-kinase complex from shed plasma membrane vesicles, J. Biol. Chem. 257 (1982) 1523–1531, https://doi.org/10.1016/s0021-9258(19)68224-4.
[4] Y. Yarden, J. Schlessinger, Epidermal growth factor induces rapid, reversible aggregation of the purified epidermal growth factor receptor, Biochemistry 26 (1987) 1443–1451, https://doi.org/10.1021/bi00379a035.
[5] Y. Yarden, J. Schlessinger, Self-phosphorylation of epidermal growth factor receptor: evidence for a model of intermolecular allosteric activation, Biochemistry 26 (1987) 1434–1442, https://doi.org/10.1021/bi00379a034.
[6] Y. Yarden, G. Pines, The ERBB network: at last, cancer therapy meets systems biology, Nat. Rev. Cancer 12 (2012) 553–563, https://doi.org/10.1038/nrc3309.
[7] R. Roskoski, The ErbB/HER family of protein-tyrosine kinases and cancer, Pharmacol. Res. 79 (2014) 34–74, https://doi.org/10.1016/j.phrs.2013.11.002.
[8] N. Papadopoulos, J. Lennartsson, The PDGF/PDGFR pathway as a drug target, Mol. Aspect. Med. 62 (2018) 75–88, https://doi.org/10.1016/j.mam.2017.11.007.
[9] E. Wåhlén, F. Olsson, O. Söderberg, J. Lennartsson, J. Heldin, Differential impact of lipid raft depletion on platelet-derived growth factor (PDGF)-induced ERK1/2 MAP-kinase, SRC and AKT signaling, Cell. Signal. 96 (2022), 110356, https://doi.org/10.1016/j.cellsig.2022.110356.
[10] P. Lajoie, I.R. Nabi, Lipid Rafts, Caveolae, and Their Endocytosis, first ed., Elsevier Inc., 2010 https://doi.org/10.1016/S1937-6448(10)82003-9.
[11] S. Sigismund, E. Argenzio, D. Tosoni, E. Cavallaro, S. Polo, P.P. Di Fiore, Clathrin-mediated internalization is essential for sustained EGFR signaling but dispensable for degradation, Dev. Cell 15 (2008) 209–219, https://doi.org/10.1016/j.devcel.2008.06.012.
[12] A. Tomas, C.E. Futter, E.R. Eden, EGF receptor trafficking: consequences for signaling and cancer, Trends Cell Biol. 24 (2014) 26–34, https://doi.org/10.1016/j.tcb.2013.11.002.
[13] R. Cabral-Dias, S. Lucarelli, K. Zak, S. Rahmani, G. Judge, J. Abousawan, L.F. Digiovanni, D. Vural, K.E. Anderson, M.G. Sugiyama, G. Genc, W. Hong, R.J. Botelho, G.D. Fairn, P.K. Kim, C.N. Antonescu, Fyn and TOM1L1 are recruited to clathrin-coated pits and regulate Akt signaling, J. Cell Biol. 221 (2022), https://doi.org/10.1083/jcb.201808181.
[14] J. Nevo, E. Mattila, T. Pellinen, D.L. Yamamoto, H. Sara, K. Iljin, O. Kallioniemi, P. Bono, P. Heikkilä, H. Joensuu, A. Wärri, J. Ivaska, Cancer therapy : preclinical mammary-derived growth inhibitor alters traffic of EGFR and induces a novel form of cetuximab resistance, 15, https://doi.org/10.1158/1078-0432.CCR-09-0773, 2009, 6570–6581.
[15] L. Bazzani, S. Donnini, A. Giachetti, G. Christofori, M. Ziche, PGE2 Mediates EGFR Internalization and Nuclear Translocation via Caveolin Endocytosis Promoting its Transcriptional Activity and Proliferation in Human NSCLC Cells, vol. 9, 2018, pp. 14939–14958.
[16] G. Sowa, Caveolae, caveolins, cavins, and endothelial cell function: new insights, Front. Physiol. 2 (JAN 2012) 1–13, https://doi.org/10.3389/fphys.2011.00120.
[17] I.H. Madshus, E. Stang, Internalization and intracellular sorting of the EGF receptor : a model for understanding the mechanisms of receptor trafficking. https://doi.org/10.1242/jcs.050260, 2009.
[18] A. Klaesson, K. Grannas, T. Ebai, J. Heldin, B. Koos, M. Leino, D. Raykova, J. Oelrich, L. Arngården, O. Söderberg, U. Landegren, Improved efficiency of in situ protein analysis by proximity ligation using UnFold probes, Sci. Rep. 8 (2018) 1–13, https://doi.org/10.1038/s41598-018-23582-1.
[19] F. Gajate, C. Mollinedo, Lipid raft isolation by sucrose gradient centrifugation and visualization of raft-located proteins by fluorescence microscopy: the use of combined techniques to assess fas/CD95 location in rafts during apoptosis triggering, in: U. Bieberich, Erhard (Eds.), (Department of Physiology, University of Kentucky Medical School, Lexington, KY (Ed.), Lipid Rafts, Methods in Molecular Biology, vol. 2187, Humana, New York, NY, 2021, pp. 147–186, https://doi.org/10.1007/978-1-0716-0814-2_9.
[20] D. Raykova, D. Kermpatsou, T. Malmqvist, P.J. Harrison, M.R. Sander, C. Stiller, J. Heldin, M. Leino, S. Ricardo, A. Klemm, L. David, O. Spjuth, K. Vemuri, A. Dimberg, A. Sundqvist, M. Norlin, A. Klaesson, C. Kampf, O. Söderberg, A method for Boolean analysis of protein interactions at a molecular level, Nat. Commun. 13 (2022) 4755, https://doi.org/10.1038/s41467-022-32395-w.

[21] H.F. Turk, R. Barhoumi, R.S. Chapkin, Alteration of EGFR spatiotemporal dynamics suppresses signal transduction, PLoS One 7 (2012), e39682, https://doi.org/10.1371/journal.pone.0039682.
[22] T. Ringerike, F.D. Blystad, F.O. Levy, I.H. Madshus, E. Stang, Cholesterol is important in control of EGF receptor kinase activity but EGF receptors are not concentrated in caveolae, J. Cell Sci. 115 (2002) 1331–1340. http://www.ncbi.nlm.nih.gov/pubmed/11884532.
[23] J. Heldin, M.R. Sander, M. Leino, S. Thomsson, J. Lennartsson, O. Söderberg, Dynamin inhibitors impair platelet-derived growth factor β-receptor dimerization and signaling, Exp. Cell Res. 380 (2019) 69–79, https://doi.org/10.1016/j.yexcr.2019.04.004.
[24] M. Yamamoto, Y. Toya, R.A. Jensen, Y. Ishikawa, Caveolin is an inhibitor of platelet-derived growth factor receptor signaling, Exp. Cell Res. 247 (1999) 380–388, https://doi.org/10.1006/excr.1998.4379.